Physiology and Molecular Biology of Plants (January 2024) 30(1):123–136
https://doi.org/10.1007/s12298-024-01413-0

RESEARCH ARTICLE

Calcium signal regulated carbohydrate metabolism in wheat seedlings under salinity stress

Ya Zhang[1] · Dan Qiao[1] · Zhe Zhang[1] · Yaping Li[1] · Shuqian Shi[1] · Yingli Yang[1]

Received: 29 August 2023 / Revised: 19 December 2023 / Accepted: 22 January 2024 / Published online: 1 February 2024

Abstract

This study aimed to explore the mechanism by which calcium (Ca) signal regulated carbohydrate metabolism and exogenous Ca alleviated salinity toxicity. Wheat seedlings were treated with sodium chloride (NaCl, 150 mM) alone or combined with 500 μM calcium chloride ($CaCl_2$), lanthanum chloride ($LaCl_3$) and/or ethylene glycol tetraacetic acid (EGTA) to primarily analyse carbohydrate starch and sucrose metabolism, as well as Ca signaling components. Treatment with NaCl, EGTA, or $LaCl_3$ alone retarded wheat-seedling growth and decreased starch content accompanied by weakened ribulose-1,5-bisphosphate carboxylation/oxygenase (Rubisco) and Rubisco activase activities, as well as enhanced glyceraldehyde-3-phosphate dehydrogenase, phosphoglycerate kinase, alpha-amylase, and beta-amylase activities. However, it increased the sucrose level, up-regulated the sucrose phosphate synthase (SPS) and sucrose synthase (SuSy) activities and *TaSPS* and *TaSuSy* expression together, but down-regulated the acid invertase (SA-Inv) and alkaline/neutral invertase (A/N-Inv) activities and *TaSA-Inv* and *TaA/N-Inv* expression. Except for unchanged A/N-Inv activities and *TaA/N-Inv* expression, adding $CaCl_2$ effectively blocked the sodium salt-induced changes of these parameters, which was partially eliminated by EGTA or $LaCl_3$ presence. Furthermore, NaCl treatment also significantly inhibited Ca-dependent protein kinases and Ca^{2+}-ATPase activities and their gene expression in wheat leaves, which was effectively relieved by adding $CaCl_2$. Taken together, $CaCl_2$ application effectively alleviated the sodium salt-induced retardation of wheat-seedling growth by enhancing starch anabolism and sucrose catabolism, and intracellular Ca signal regulated the enzyme activities and gene expression of starch and sucrose metabolism in the leaves of sodium salt-stressed wheat seedlings.

Keywords Sodium salt stress · Calcium signal · Carbohydrate metabolism · Wheat seedling

Introduction

The growth and development of plants are related to a series of complex energy-consuming reactions driven by photosynthetic reaction products. Because photosynthesis products starch and sucrose are the main source of carbon and energy for plant metabolism (Liu et al. 2020). Changes in the amount of starch and soluble sugars including sucrose reflect carbohydrate metabolism and plant carbon requirement under abiotic stress. Salinity stress can promote starch hydrolysis and thus increases the accumulation of sucrose and total sugars in various plants (Li et al. 2023; Meng et al. 2023). Accordingly, a close relationship between the metabolism of starch and sucrose has been suggested. A series of synthetases, such as glyceraldehyde-3-phosphate dehydrogenase (GAPDH), Rubisco activase (RCA), ribulose-1,5-bisphosphate carboxylase/oxygenase (Rubisco), phosphoglycerate kinase (PGK), sucrose synthase (SuSy), and sucrose phosphate synthase (SPS), as well as the degradative enzymes amylase and invertase (Inv) play an important function in the metabolism of carbohydrate starch and sucrose (Sui et al. 2015; Yan et al. 2021; Elsayed et al. 2022; Yu et al. 2022). Several recent studies showed that salinity stress significantly inhibits Rubisco and RCA activities in rice seedlings (Yan et al. 2021), and that PGK transcript level notably decreases in sodium salt-stressed rapeseed plants (ElSayed et al. 2022). Ju et al. (2021) also found that the activities of SPS and SuSy significantly enhance but soluble acid invertase (SA-Inv) activity decreases in cotton-boll leaves under sodium salt exposure. Transcriptome analysis

✉ Yingli Yang
xbsfxbsdyang@163.com

[1] School of Life Science, College of Life Science, Northwest Normal University, Lanzhou 730070, Gansu, People's Republic of China

further reveals that under sodium chloride (NaCl) treatment, the expression of SPS, SuSy, alpha-amylase (α-amylase), and beta-amylase (β-amylase) genes is notably promoted in salt-tolerant oat cultivar, whereas SuSy gene expression is down-regulated in salt-sensitive ones (Xu et al. 2021). Even though a number of studies have investigated carbohydrate metabolism in various plants, the regulatory mechanism of plant resistance to salinity stress associated with the synthesis and decomposition of starch and sucrose remains unclear.

Currently, salinization affects about 20% of the world's cultivated land, and an additional 2 million hectare (about 1%) is deteriorated by salinity annually (Qiu et al. 2017; Ke et al. 2018), thereby seriously threating ecological environment and agricultural production. Furthermore, projection indicates that 50% of all arable land will be affected by salt within the mid of the twenty-first century (Miceli et al. 2021). The depressive effect of salinity on plant growth may result from altering various metabolism and physiological processes (Patel et al. 2023; Dinler et al. 2023). The pivotal role of calcium (Ca) is involved in the normal growth and development of plants, as well as plant response to abiotic stress. Some researchers have found that exogenous Ca application can alleviate many plant symptoms caused by sodium salt stress (Manishankar et al. 2018; Roy et al. 2019). Recently, Kamran et al. (2021) reported that exogenous calcium chloride ($CaCl_2$) can significantly promote starch synthesis in plant seedlings under sodium salt stress. Although Ca signal-mediated plant responses to salinity environment have been focused (Manishankar et al. 2018; Bachani et al. 2022), few studies have revealed the Ca-alleviating mechanism on salinity toxicity through studying photosynthetic carbon metabolism. Moreover, the relationship between starch or sucrose metabolism and plant salt tolerance has also received different views (Kerepesi and Galiba 2000; Sui et al. 2015; Shen et al. 2019). Our previous studies have found that NaCl treatment (concentration > 100 mM) causes obvious phytotoxicity in different wheat varieties (Yang et al. 2010; Zhang et al. 2020). Importantly, moderate Ca concentrations can effectively enhance wheat-seedling tolerance to 150 mM NaCl treatment, as demonstrated by the enhanced growth of NaCl + $CaCl_2$-treated wheat seedlings (data not shown). We hypothesized that exogenous Ca presence could relieve NaCl-induced phytotoxicity by altering carbohydrate sucrose and starch metabolism, thus mitigating growth restriction. Accordingly, wheat seedlings were exposed to 150 mM NaCl, 500 μM lanthanum chloride ($LaCl_3$), 500 μM ethylene glycol tetraacetic acid (EGTA), and 500 μM $CaCl_2$ alone or in combination, and then carbohydrate starch and sucrose metabolism, the related enzyme activity and gene expression, and the Ca signal components in wheat leaves were evaluated. The present study may be beneficial for agriculture practices in developing the technology of mitigating NaCl toxicity and replenishing new knowledge of salt tolerance mechanism.

Materials and methods

Culture and treatment of wheat seedlings

Wheat cultivar Xihan3 seeds were bred by Gansu Agricultural University. Disinfection of seeds and cultivation of the seedlings were perfected according to Zhang et al. (2021). Seedling treatment were set as follows: control, 150 mM NaCl, 500 μM $LaCl_3$, 500 μM EGTA, 150 mM NaCl + 500 μM $CaCl_2$, 150 mM NaCl + 500 μM $CaCl_2$ + 500 μM $LaCl_3$, 150 mM NaCl + 500 μM $CaCl_2$ + 500 μM EGTA, and at least three replicates were for each treatment. One-fourth Hoagland solution was used to cultivate untreated seedlings, and NaCl, $CaCl_2$, $LaCl_3$, and EGTA were dissolved in one-fourth Hoagland solution to treat wheat seedlings. The culture medium was renewed every 2 days.

Measurement of growth and biomass

Fifteen wheat seedlings grown for 6 days were arbitrarily inspected from each treatment group to measure the root and stem lengths (cm). The underground and above-ground parts of the seedlings were weighed for fresh weight (FW). Subsequently, the different parts of the seedlings were baked for 10 min at 105 °C and then at 80 °C for constant weight recorded as dry weight (DW).

Analyses of carbohydrate content

The amount of total soluble sugar, sucrose, and starch was measured according to Ju et al. (2021). Dried wheat leaves (0.1 g) were extracted with 5 mL distilled water and bathed at 80 °C for 30, 20, and 20 min successively. Three extracts were collected and dissolved to 25 mL to determine the amount of soluble total sugar and sucrose. The extract (1 mL) was mixed with 4 mL of anthrone and heated for 10 min in boiling water. The temperature of the mixture dropped to room temperature to measure the absorbance at 625 nm, and the amount of total soluble sugar was calculated. The extract (400 μL) was mixed with 500 mM sodium hydroxide (NaOH) solution to reduce the interference of fructose as much as possible. After it was bathed in boiling water for 5 min and cooled to room temperature, 2.8 mL of hydrochloric acid (30%) solution and 800 μL of resorcinol solution (0.1%) were added successively. The mixture was incubated again at 80 °C for 10 min. The absorbance at 485 nm was detected to calculate sucrose content.

Starch amount was determined according to Liu et al. (2013). After the total soluble sugar was extracted, the residue of wheat leaves was extracted with 3 mL of distilled water and bathed at 100 °C for 15 min. It was cooled to room temperature and mixed with 9.2 M perchloric acid (2 mL), and diluted to 10 mL volume with distilled water. Centrifugation was perfected at 4000 r for 10 min to obtain the supernatant. Subsequently, the residue was extracted with 4.6 M perchloric acid (2 mL) again, and distilled water was added to reach the total volume of 10 mL. After centrifuging at 4000 r for 10 min, the supernatant from twice centrifugation was combined and dissolved to 25 mL, which was the extract solution for detecting the amount of starch by recording the absorbance at 625 nm.

Detection of enzyme activities related to photosynthetic carbon assimilation

Crude enzyme solution for the measurement of Rubisco activity was extracted as described by Gao (2006). Wheat leaves (0.3 g) were ground with 2 mL of 40 mM tris (hydroxymethyl) aminomethane (Tris)-hydrochloride (HCl) buffer (pH 7.6) supplying 5 mM glutathione (GSH), 250 μM ethylenediamine tetraacetic acid (EDTA) and 10 mM magnesium chloride ($MgCl_2$). After centrifuging at 15,000×*g* for 15 min, the supernatant was collected as enzyme solution. According to a modified method of Kumar et al. (2016), the enzyme extract (100 μL) was mixed with the reaction solution (2.8 mL) comprising 50 mM Tris–HCl (pH 7.8), 800 μM EDTA, 6 mM $MgCl_2$, 3.57 mM creatine phosphate, 357 μM reduced nicotinamide adenine dinucleotide (NADH), 5 mM sodium bicarbonate ($NaHCO_3$), 3.57 mM adenosine triphosphate (ATP), 6 $U{\cdot}L^{-1}$ creatine phosphate, 6 $U{\cdot}L^{-1}$ 3-PGK and 6 $U{\cdot}L^{-1}$ 3-phosphoglyceraldehyde dehydrogenase (PGD). A background rate of NADH oxidation as the initial activity was determined by monitoring the absorbance at 340 nm. Afterwards, 25 mM ribulose-1,5-bisphosphate (100 μL) was used to initiate the reaction, and the change in absorbance was determined at 340 nm for 3 min. Ribulose-1,5-bisphosphate carboxylase/oxygenase activity was represented by $U{\cdot}g^{-1}$ FW based on NADH oxidation.

Rubisco activase activity was measured according to Kumar et al. (2016) with some modification. Wheat leaves (0.1 g) were ground with 1.9 mL of 50 mM Tris–HCl (pH 7.8) supplying 0.01% (v/v) polyethylene glycol octyl phenyl ether (Triton X-100), 10 mM $MgCl_2$, 1 mM EDTA, and 10 mM DTT. The supernatant (100 μL) obtained by centrifuging at 15,000×*g* for 15 min was combined with 50 mM Tris–HCl buffer (pH 7.8, 1300 μL) containing 357 μM of NADH, 3.57 mM of ATP, 14.29 mM of $NaHCO_3$, 6 mM of $MgCl_2$, 200 μM of EDTA-Na_2, and 5.71 $U{\cdot}mL^{-1}$ of creatine phosphokinase, glycerate phosphomyase, and glyceraldehyde phosphate dehydrogenase. Rubisco activase activity was determined based on ADP production in an ATP-dependent reaction by monitoring the absorbance at 340 nm.

Glyceraldehyde-3-phosphate dehydrogenase and PGK activities were detected based on the modified methods of Wang et al. (2012). The crude enzyme solution was prepared as follows: plant material (0.5 g) was blended with 2 mL of 100 mM 4-(2-hydroxyethyl)-1-piperazineethanesulfonic acid (HEPES)–NaOH buffer (pH 7.8) supplying 100 μM EDTA, 10% polyvinylpyrrolidone, 100 mM ascorbic acid, and 8 mM $MgCl_2$. The supernatant (20 μL) obtained by centrifuging at 15,000×*g* for 15 min was blended with 100 μL of the reaction solution comprising 50 mM HEPES–NaOH buffer (pH 7.8), 10 mM $MgCl_2$, 5 mM ATP, 200 μM nicotinamide adenine dinucleotide phosphate (NADPH), 1 mM EDTA, 4 U triosephosphate isomerase, and 20 U PGK. Changes in the absorbance based on NADPH oxidation was monitored at 340 nm for 1 min to determine GAPDH activity. Meanwhile, PGK activity was measured by replacing NADPH and PGK in the reaction solution with NADH and 3 U GAPDH, respectively.

A modification of the method of Hajihashemi et al. (2020) was used to extract enzyme solution. Wheat leaves (0.5 g) were ground with 10 mL of ice-cold distilled water, stored at room temperature for 15 min, and shaken every few minutes. It was centrifuged (10 min) at 3000 r to collect the supernatant for detecting amylase activities according to Li et al. (2013) with some modifications. The enzyme extract (1 mL) for measuring α-amylase activity was incubated at 70 °C for 15 min to inactivate β-amylase. It was mixed with 1 mM citrate buffer (pH 5.6, 2 mL) supplying 1% soluble starch and stored at 40 °C for 5 min. Afterwards, 44 mM 3,5-dinitrosalicylic acid (DNS) reagent (2 mL) containing 400 μM NaOH and 1 M sodium potassium tartrate was added and bathed at 40 °C for 5 min, and then the solution was cooled to room temperature. The mixed solution was diluted to 10 mL with distilled water. In the control tube, 400 μM NaOH and 1 M sodium potassium tartrate without DNS was mixed with the reaction solution. The absorbance at 540 nm was measured, and α-amylase activity was calculated according to the standard curve of maltose and denoted by mg $maltose{\cdot}h^{-1}{\cdot}g^{-1}$ FW. Except that the enzyme extract did not need to passivate β-amylase, a similar process was used to determine total amylase activity. Beta-amylase activity was obtained by subtracting the activity of α-amylase from the activity of total amylase.

Detection of enzyme activities related to sucrose metabolism

Sucrose phosphate synthase and SuSy activities were determined according to Winter and Huber (2000) and Shu et al. (2009). Wheat leaves (0.3 g) were ground with

3 mL of 50 mM HEPES–NaOH buffer (pH 7.5), left at 4 °C for 30 min, and centrifuged (10 min) at 10,000×*g*. Ammonium sulphate solution was blended with the supernatant to achieve saturation above 80%. After it was centrifuged again, the precipitate was completely dissolved with 50 mM HEPES–NaOH buffer (pH 7.5, 1 mL), and crude enzyme extract was obtained to detect SPS and SuSy activities. The reaction system for measuring enzyme activity comprised crude enzyme extract (50 µL), 15.63 mM HEPES–NaOH buffer (pH 7.5), 6.25 mM $MgCl_2$, 18.75 mM uridine diphosphate glucose and 6.25 mM fructose 6-phosphate or fructose. After it was bathed at 30 °C for 30 min, 2 M NaOH (200 µL) was used over the reaction, and the mixture for the determination of enzyme activity was obtained. Then, 360 µL of the mixture was combined with 2 M NaOH (200 µL) and heated at 100 °C for 5 min before adding 3% hydrochloric acid (2.8 mL) and 0.1% resorcinol (800 µL) successively. The absorbance at 485 nm was determined after it was bathed at 80 °C for 10 min. The above reaction systems containing fructose 6-phosphate or fructose were used to detect the activities of SPS and SuSy. The amount of the reaction products sucrose-6-phosphate (sucrose-p) and sucrose were calculated according to their standard curve, respectively. The units of these two enzyme activities were denoted as µmol sucrose-p·h^{-1}·mg^{-1} protein and µmol sucrose·h^{-1}·mg^{-1} protein, respectively.

Acid invertase and A/N-Inv activities were analyzed consulting the method of Hu et al. (2018) and Meng et al. (2023) with some modification. Wheat leaves (0.2 g) were pulverised with 4 mL of 150 mM potassium phosphate buffer (PBS, pH 7.5) supplying 0.1% β-mercaptoethanol, 5 mM $MgCl_2$, 0.05% bovine serum albumin (BSA) and 0.05% Triton-X100, and left at 4 °C for 20 min. The supernatant acquired by centrifuging at 12,000×*g* for 30 min was blended with ammonium sulphate solution to achieve the saturation above 80%. After it was centrifuged again, the precipitate was fully dissolved with 15 mM PBS buffer (pH 7.5, 1 mL) containing 0.01% β-mercaptoethanol, 250 µM $MgCl_2$, and 0.05% BSA. Then, the crude enzyme solution for detecting SA-Inv and A/N-Inv activities was obtained. The reaction systems for the measurement of SA-Inv activity comprised 100 µL of crude enzyme solution, 56 mM sodium acetate buffer (pH 4.5), and 20 mM sucrose, and bathed at 37 °C for 30 min, which was stopped by adding 1.5 mL of DNS reagent and boiling at 100 °C for 5 min. The solution was cooled to room temperature, and its absorbance at 540 nm was recorded. Different from the detection of SA-Inv activity, A/N-Inv activity was measured using sodium acetate buffer (pH 7.3). Enzyme activity was determined according to a glucose standard curve and represented by µmol glucose·h^{-1}·mg^{-1} protein.

Detection of soluble protein content

According to the method of Rekowski et al. (2021), the amount of soluble protein was determined and calculated based on the standard curve of BSA.

Analysis of real-time polymerase chain reaction (PCR)

Total RNA was extracted as described by Zhang et al. (2021). Wheat leaves were pulverised in liquid nitrogen and lysed with 1 mL of RNAiso Plus. PrimeScriptTM RT Reagent Kit with gDNA Eraser (PerfectReal Time) (Takara, Purchased from Shanghai Baise Biotechnology Co., Ltd.) was used to synthesise cDNA. Sequence-specific primers of wheat related genes (Table 1) were designed, using Primer Premier 5.0 software and synthesised by Shanghai Shenggong Bioengineering Co., Ltd. The reaction system and reaction conditions of qRT-PCR were set in accordance with a SYBR Premix Ex TaqTM Kit, and three parallel genes were set for each treatment. The internal reference gene was wheat glyceraldehyde-3-phosphate dehydrogenase gene (*TaGAPDH*), and the relative expression of genes was analysed according to the $2^{-\Delta\Delta Ct}$ method.

Determination of Ca-dependent protein kinase (CDPK) and Ca^{2+}-ATPase activities

According to Zhang et al. (2022), wheat leaves were homogenised with phosphate buffer, and then the tissue cells in the homogenate were lysed by ultrasonication. The supernatant was collected by centrifuging at 5000×*g* and 4 °C for 10 min, and the activities of CDPK and Ca^{2+}-ATPase were analysed using enzyme-linked immunosorbent assay

Table 1 Primers used for RT-qPCR

Primer	Sequence (5′–3′)
TaGAPDH	F: TTAGACTTGCGAAGCCAGCA
	R: AAATGCCCTTGAGGTTTCCC
TaSPS	F: ATCGTCACGCTCGCTCAA
	R: AGTCATCTTCCTGCCAAAATTACA
TaSuSy	F: CCGACAAGGAGAAGTATG
	R: CGAGTTCACTAACATTCAC
TaSA-Inv	F: AACGTCACAAGGCTCGTCGT
	R: ATGTAGGCCTGATTGTAGGAGGAGT
TaA/N-Inv	F: CACTGGAGCGTAAGAGGTCATT
	R: CCACACTATCAAAGCCGTCAT
TaCDPKs	F: GGACCTGAGTCGGATGTTTGG
	R: CCCTTGGGTTCTTCACCAGTAA
TaCa^{2+}-ATPase	F: CCACCGTCATCTGCTCCGAC
	R: ATTGCACACAGCTGCGACCT

(ELISA). ELISA kits were ordered from Shanghai Enzyme Linked Biotechnology Co., Ltd.

Statistical analysis

Experimental data were analyzed with SPSS 20.0 software. After analysis of variance (one-way ANOVA), Duncan's multiple comparisons were performed and significant differences between treatment groups were assessed with different lowercase letters ($P \leq 0.05$). Experimental data were represented by the average value ± standard error (SE) of biological triplicates. Figures were made with Origin 2021 software.

Results and discussion

Changes in growth and biomass of wheat seedlings

As shown in Fig. 1A, B, treatment with 150 mM NaCl, 500 μM $LaCl_3$ or 500 μM EGTA alone significantly restricted the growth of shoots and roots, and the inhibitory effect of NaCl, $LaCl_3$, or EGTA weakened, successively. Adding 500 μM $CaCl_2$ to NaCl-stressed seedlings effectively promoted seedling growth with about 32% and 67% increase of shoot length and root length, respectively, compared with sodium salt exposure alone. Notably, 500 μM $LaCl_3$ or EGTA application blocked the promotion of seedling growth under NaCl + $CaCl_2$ treatment, and the effect of EGTA was weaker than that of $LaCl_3$. Additionally, FW and DW of the stems and roots obviously decreased under NaCl, $LaCl_3$ or EGTA treatment alone, with the maximum reduction due to NaCl stress (Fig. 1C, D). Compared with the control, these two parameters of seedling stem decreased by about 58% and 55% under 150 mM NaCl, and significantly decreased by about 45% and 27%, 27% and 18% under 500 μM $LaCl_3$ or 500 μM EGTA exposure alone, respectively. Adding 500 μM $CaCl_2$ effectively prevented the sodium salt-induced reduction of biomass, as demonstrated by the 38% and 40% increase in FW and DW of seedling shoots and by about 43% and 39% elevation in these two parameters of the roots, respectively, compared with NaCl stress alone. The 150 mM NaCl + 500 μM $CaCl_2$-induced change of seedling biomass was blocked by $LaCl_3$ or EGTA, and the effect of EGTA was weaker than that of $LaCl_3$. Lanthanum chloride is an inhibitor of plasma membrane Ca channels, and EGTA can chelate cell-wall-related or extracellular Ca^{2+} (Bai et al. 2013). These results suggested that the transport of extracellular Ca into the cells was related to the regulation of seedling growth and that exogenous $CaCl_2$ application could relieve salinity toxicity in wheat seedlings. By contrast, *Solanum lycopersicum* L. seedlings grow well under 30 μM $LaCl_3$ treatment alone (Huang and Shan 2018), and 1.5 mM EGTA alone insignificantly affect the growth of *Brassica napus* L. seedlings (Nawaz et al. 2019), indicating the growth of these plants seems to be independent of extracellular Ca transport. Additionally, the changes of biomass, especially DW, implied that different treatments may result in the alteration in the production of photosynthetic products in wheat seedlings (Kerepesi and Galiba 2000).

Changes in carbohydrate content of wheat leaves

Starch and sucrose are photosynthetic products. Compared with untreated wheat leaves, the leaves exposed to 150 mM NaCl or 500 μM $LaCl_3$ alone exhibited an obvious increase of the amount of total soluble sugar and sucrose, as well as a marked decrease in starch content (Table 2). By contrast, treatment with 500 μM EGTA alone did not affect the amount of total soluble sugar but increased sucrose content by 39% and decreased starch level by 18% compared with the control. Carbohydrates starch and sucrose are involved in energy supply and osmotic adjustment when plants are exposed to salinity environment (Shen et al. 2019). Some researchers believe that starch and sucrose metabolism play pivotal roles in determining the ability of the salt tolerance of various plants (Wang et al. 2013; Pan et al. 2021). In particular, the accumulation of soluble sugar, primarily sucrose, is associated with enhanced plant survivability to abiotic stress (Kerepesi and Galiba 2000). The changes of sugar contents in wheat leaves confirmed the inhibition of starch synthesis and sucrose degradation under individual NaCl, $LaCl_3$ or EGTA treatment. However, such changes weakened the energy mobilization and could not meet the energy requirement of wheat-seedling growth, thus diminishing the length and biomass of stems and roots under individual NaCl, $LaCl_3$ or EGTA treatment. Several previous research also showed the accumulation of various soluble sugars including sucrose, the decline of starch content, and the improvement of salt tolerance in various plants (Gao et al. 2019; Li et al. 2023; Zhang et al. 2023). On the contrary, NaCl treatment promotes the accumulation of starch in the leaves of *Cucumis sativus* L. (Zhu et al. 2016) and in the chloroplasts of *C. sativus* L. mesophyll cells (Shen et al. 2019). The present results also implied that the transmembrane transport of extracellular Ca might be associated with the regulation of starch and sucrose metabolism in wheat leaves under salinity stress. Furthermore, adding 500 μM $CaCl_2$ effectively blocked NaCl-induced changes in the amount of these three parameters (Table 2), with about 12% and 41% reduction of total soluble sugar and sucrose contents and about 78% enhancement of starch level, respectively, as compared with sodium salt treatment alone. This further suggested that extracellular Ca transport and even Ca signal might

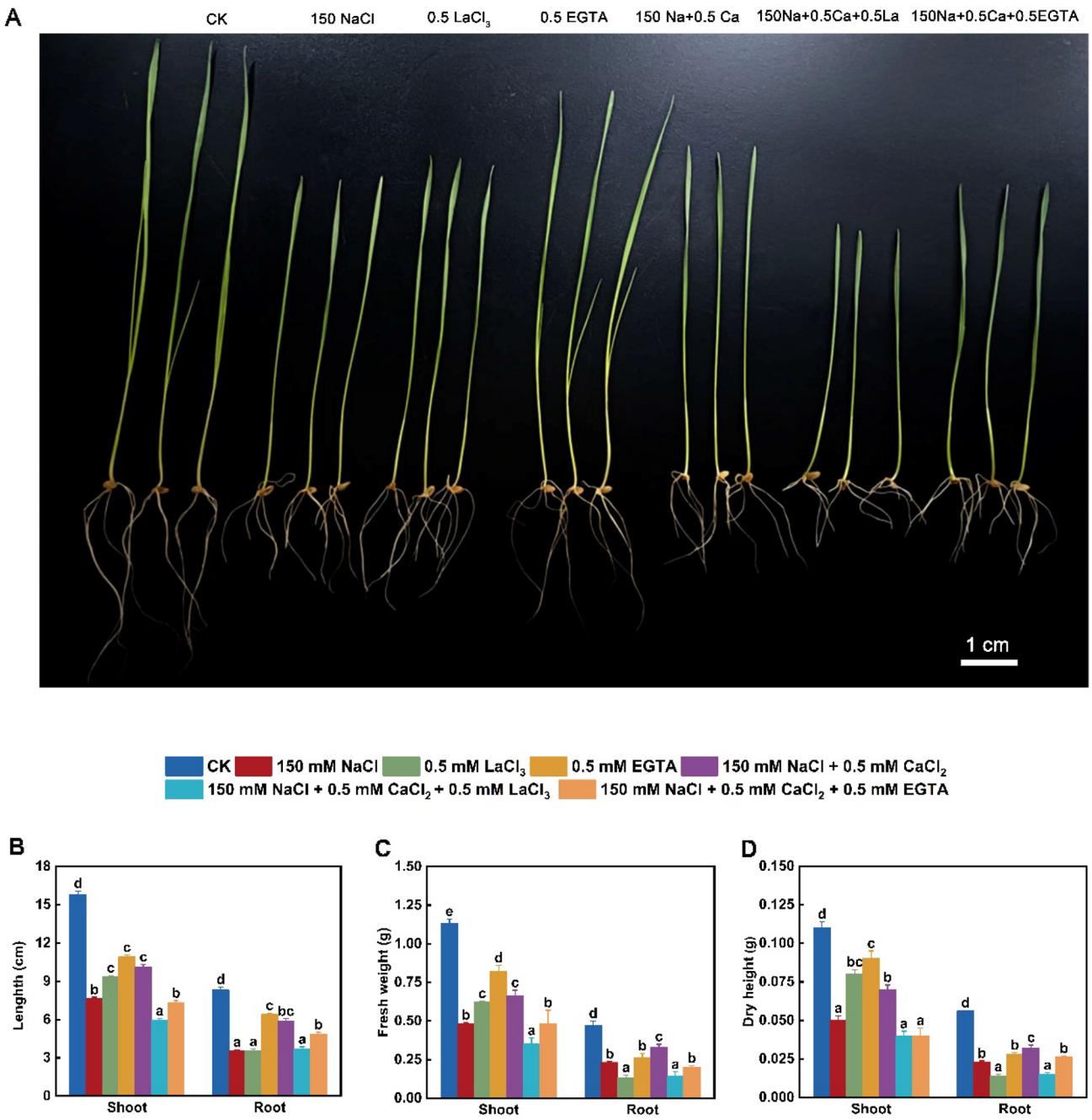

Fig. 1 Changes in growth (**A**, **B**) and biomass (**C**, **D**) of wheat seedlings under different treatments. Control (CK); lanthanum chloride ($LaCl_3$); ethylene glycol tetraacetic acid (EGTA). Data are the means of three replicates (± SE). Different lowercase letters indicate significant difference between samples according to Duncan's new multiple-range test ($P < 0.05$)

be involved in the enhancement of sucrose degradation and starch synthesis, which was beneficial to providing more energy for wheat seedling under $NaCl + CaCl_2$ treatment. These suggestions can be supported by several previous observations, which showed that the ability of more starch accumulation may provide greater energy for *T. halophila* to resist the damaging effects of high salinity (Wang et al. 2013), and that the melatonin-alleviated effect on salt stress occurred with increased starch accumulation in *Medicago sativa* L. (Li et al. 2022c). More importantly, the involvement of predicted Ca function in seedling growth and sugar metabolism was demonstrated by further investigation. Herein, the presence of $LaCl_3$ significantly eliminated the $NaCl + CaCl_2$-induced effects on these three parameters, resulting in about 25% and 164% increases of total soluble sugar and sucrose

Table 2 Changes in carbohydrate content in wheat leaves under different treatments

Treatments	Starch (mg·g^{-1} DW)	Sucrose (mg·g^{-1} DW)	Total soluble sugar (mg·g^{-1} DW)
CK	12.31 ± 0.17d	6.33 ± 0.15a	15.84 ± 0.45a
150 mM NaCl	7.21 ± 0.14a	8.43 ± 0.16b	24.88 ± 0.69d
0.5 mM $LaCl_3$	8.38 ± 0.26b	9.18 ± 0.18b	18.62 ± 0.60b
0.5 mM EGTA	10.12 ± 0.19c	8.80 ± 0.20b	16.69 ± 0.38a
150 mM NaCl + 0.5 mM $CaCl_2$	12.81 ± 0.13d	4.97 ± 0.14a	21.85 ± 0.34c
150 mM NaCl + 0.5 mM $CaCl_2$ + 0.5 mM $LaCl_3$	7.59 ± 0.19a	13.11 ± 0.17c	27.33 ± 0.81e
150 mM NaCl + 0.5 mM $CaCl_2$ + 0.5 mM EGTA	6.94 ± 0.22a	10.76 ± 0.11c	25.45 ± 0.62d

Control (CK); lanthanum chloride ($LaCl_3$); ethylene glycol tetraacetic acid (EGTA). Data are the means of three replicates (±SE). Different lowercase letters indicate significant difference between samples according to Duncan's new multiple-range test ($P < 0.05$)

contents, respectively, along with about 41% reduction in starch content. Additionally, the levels of total soluble sugar and sucrose under NaCl + $CaCl_2$ + EGTA treatment increased by about 16% and 116%, respectively, whereas the amount of starch decreased by about 46%, when compared with those of NaCl + $CaCl_2$ exposure (Table 2).

Changes in enzyme activities related to starch metabolism in wheat leaves

As shown in Fig. 2A–D, the activities of Rubisco and RCA significantly down-regulated and those of GAPDH and PGK up-regulated in wheat leaves under 150 mM NaCl, 500 µM

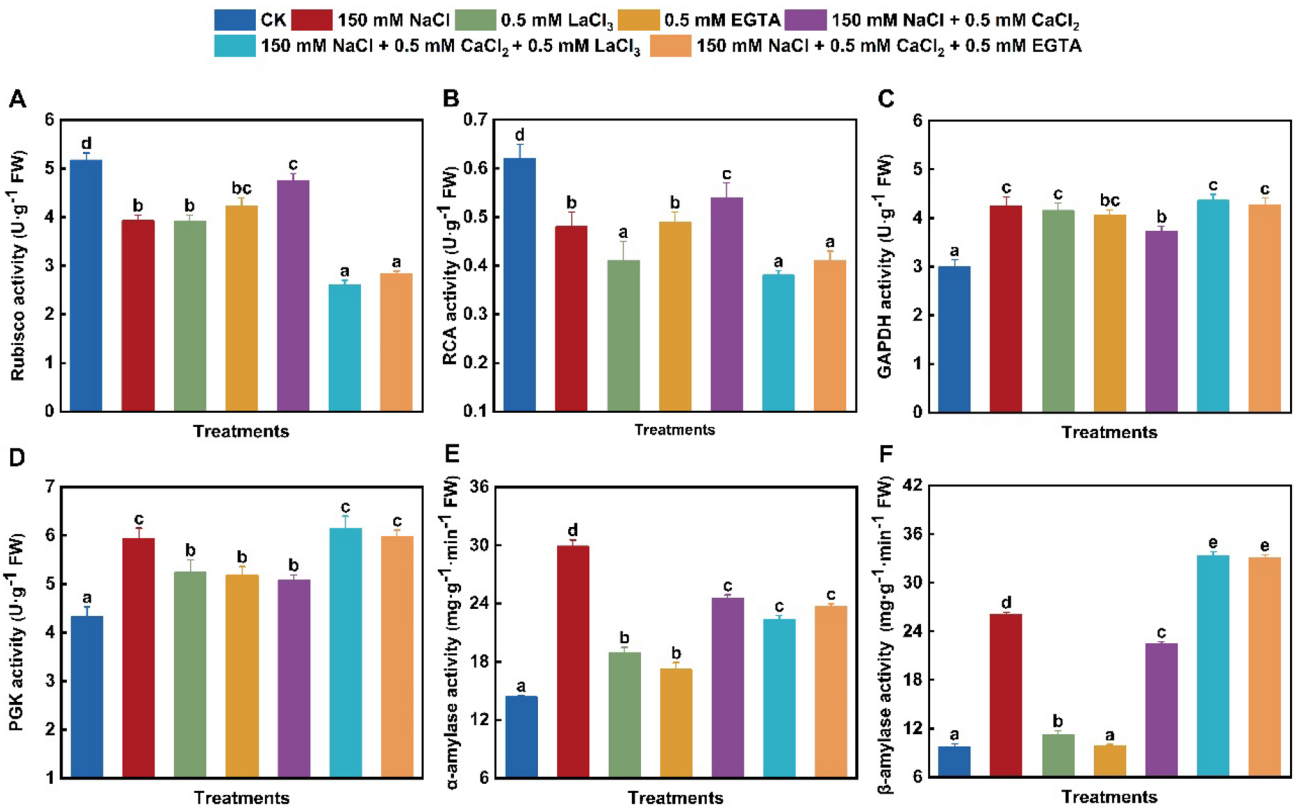

Fig. 2 Changes in enzyme activities related to starch metabolism in wheat leaves under different treatments. **A** Ribulose-1,5-bisphosphate carboxylation/oxygenase (Rubisco) activity; **B** Rubisco activase (RCA) activity; **C** glyceraldehyde-3-phosphate dehydrogenase (GAPDH) activity; **D** phosphoglycerate kinase (PGK) activity; **E** alpha-amylase (α-amylase) activity; **F** beta-amylase (β-amylase) activity. Control (CK); lanthanum chloride ($LaCl_3$); ethylene glycol tetraacetic acid (EGTA). Data are the means of three replicates (±SE). Different lowercase letters indicate significant difference between samples according to Duncan's new multiple-range test ($P < 0.05$)

$LaCl_3$, or 500 µM EGTA exposure alone. Starch synthesis through the Calvin cycle depend on Rubisco, RCA, PGK, and GAPDH in plant chloroplasts (Xia et al. 2009; ElSayed et al. 2022). Several previous observations also showed the significant inhibition of Rubisco and RCA activities (Yan et al. 2021) and the obvious increase of GAPDH activity (ElSayed et al. 2022) in various plants under sodium salt stress. The present findings might suggest the weakening of the fixed utilization of CO_2 and thus reduced starch content through decreasing Rubisco and RCA activities in wheat leaves under NaCl, $LaCl_3$ and EGTA exposure alone. Meanwhile, these results also confirmed that the transmembrane transport of extracellular Ca was involved in the regulation of enzyme activities related to starch synthesis, and implied that NaCl-induced reduction of starch content might result from the weakening of Ca transfer into cells in wheat leaves. Differently, the activity of RCA in *Solanum lycopersicum* L. leaves significantly enhances initially and then gradually weakens with increased NaCl concentration (Li et al. 2022b). And also, the stimulation of Rubisco and the inhibition of PGK are caused in *O. sativa* leaves by NaCl treatment (Wei et al. 2021).

Amylase catalyzes the degradation of starch, and even the change of its activity is associated with the regulation of sucrose and starch content in plants (Xing et al. 2023). Wheat leaves under NaCl, $LaCl_3$, and EGTA treatment alone displayed different changes in the activities of α-amylase and β-amylase (Fig. 2E, F). Compared with the control, these two enzyme activities were notably stimulated with about 108% and 168% enhancement under 150 mM NaCl alone, respectively. Similarly, exposure with 500 µM $LaCl_3$ alone promoted the activities of α-amylase and β-amylase by 132% and 116%, respectively (Fig. 2E, F). By contrast, 500 µM EGTA treatment alone obviously increased α-amylase activity to about 119% of the control, but unaltered β-amylase activity (Fig. 2E, F). And also, the $LaCl_3$- or EGTA-alone-induced effect on amylase activity was weaker than the NaCl-alone-induced one. Such changes seemed to indicate that the enhancement of starch degradation by α-amylase and β-amylase might depend on the transport of extracellular Ca in wheat leaves. This speculation is supported by similar observation in *Rosa chinensis* leaves (Li et al. 2022a), and the opposite changes of β-amylase activity and starch level in *C. sativus* L. leaves (Shen et al. 2019) under sodium salt stress.

Compared with 150 mM NaCl alone, the activities of Rubisco and RCA predominantly increased by 21% and 33%, respectively, whereas those of GAPDH and PGK obviously decreased by 12% and 14% in salinity-stressed seedlings in the presence of 500 µM $CaCl_2$ (Fig. 2). Compared with the combined treatment of NaCl and $CaCl_2$, NaCl + $CaCl_2$ + 500 µM $LaCl_3$ resulted in about 45% and 44% decrease of Rubisco and RCA activities, but about 17% and 21% increase of GAPDH and PGK activities, respectively (Fig. 2A–D). Adding 500 µM EGTA also effectively attenuated the altered activities of these four enzymes under the combined treatment of NaCl and $CaCl_2$. And also, the application of 500 µM $CaCl_2$ partially blocked the sodium salt-induced enhancement in α-amylase and β-amylase activities, with about 18% and 14% down-regulation compared with NaCl treatment alone, respectively (Fig. 2E, F). Compared with 150 mM NaCl + 500 µM $CaCl_2$ exposure, adding 500 µM $LaCl_3$ or 500 µM EGTA obviously stimulated β-amylase activity but did not affect α-amylase activity in NaCl + $CaCl_2$-treated seedlings (Fig. 2E, F). More recently, Yang et al. (2022) reported that trehalose can weaken the salinity-inhibitory effect on starch synthesis by enhancing Rubisco and GAPDH activities in *Solanum lycopersicum* L. leaves. Moreover, Li et al. 2022b) considered that the maintenance of Rubisco activity is correlated with the high tolerance of *Suaeda salsa* L. to salt environment. In the present study, the modification of these enzyme activities further suggested that Ca is an important regulator of starch metabolism, and that increased starch level depend on enhanced starch synthesis by Rubisco and RCA and weakened starch hydrolysis by β-amylase in the leaves of NaCl + $CaCl_2$-treated wheat seedlings. Similarly, exogenous Ca addition down-regulates α-amylase activity and starch degradation in *O. sativa* seedlings under fluoride stress (Singh et al. 2021). However, exogenous $CaCl_2$ presence enhances α-amylase and β-amylase activities and thus reduces starch accumulation in *Chenopodium quinoa* Willd. seeds (Hajihashemi et al. 2020) and rice leaves (Meng et al. 2023) under sodium salt stress. Therefore, the alleviation of sodium salt toxicity due to exogenous $CaCl_2$ application might be associated with enhanced starch synthesis and weakened starch degradation by altering Rubisco, RCA, and amylase activities in wheat leaves under salinity stress.

Changes in enzyme activities and gene expression related to sucrose metabolism in wheat leaves

Under 150 mM NaCl stress, the activities of SPS and SuSy in wheat leaves significantly increased to 144% and 134% of the control, whereas SA-Inv and A/N-Inv activities notably decreased to 65% and 78% of the control, respectively (Fig. 3). Except for unchanged A/N-Inv activity, the 500 µM $LaCl_3$-induced effects on SPS, SuSy, and SA-Inv were similar to NaCl-caused ones. By contrast, under treatment with 500 µM EGTA alone, SPS and A/N-Inv activities remained unchanged, whereas the activity of SuSy or SA-Inv notably elevated or decreased to 131% or 77% of the control, respectively (Fig. 3). And also, NaCl stress alone notably promoted the expression of *TaSPS* by about 94% and 91% and *TaSuSy* by about 67% and 26% at 2 and 6 days compared with the control, respectively (Fig. 4A, B). However, salinity stress

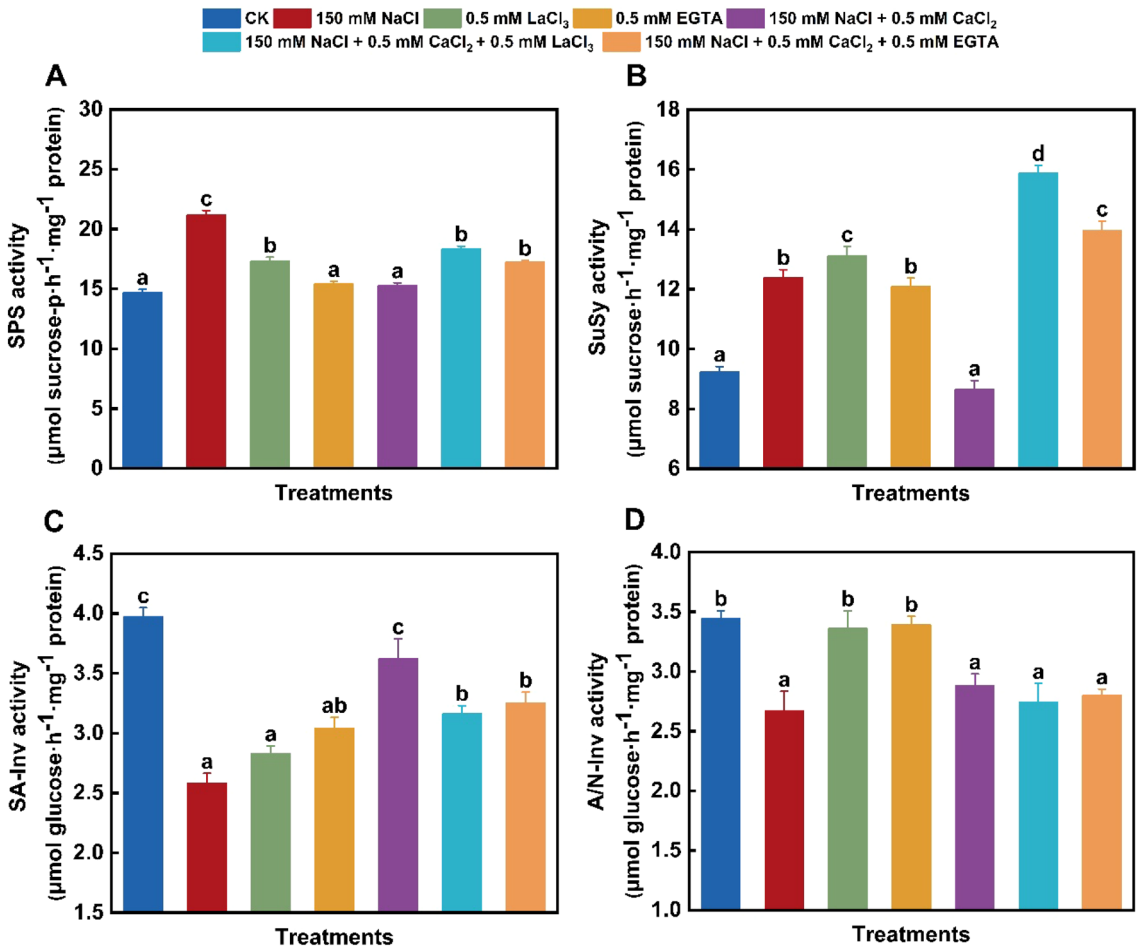

Fig. 3 Changes in enzyme activities related to sucrose metabolism in wheat leaves under different treatments. **A** Sucrose phosphate synthase (SPS) activity; **B** sucrose synthase (SuSy) activity; **C** soluble acid invertase (SA-Inv) activity; **D** alkaline/neutral invertase (A/N-Inv) activity. Control (CK); lanthanum chloride ($LaCl_3$); ethylene glycol tetraacetic acid (EGTA). Data are the means of three replicates (±SE). Different lowercase letters indicate significant difference between samples according to Duncan's new multiple-range test ($P < 0.05$)

obviously suppressed the expression of *TaSA-Inv* and *TaA/N-Inv* in wheat leaves (Fig. 4C, D). By contrast, *TaSPS* gene expression was promoted due to 500 μM $LaCl_3$ exposure alone but remained unaltered to 500 μM EGTA exposure, while the expression of *TaSuSy* significantly up-regulated due to individual $LaCl_3$ or EGTA treatment (Fig. 4A, B). And also, *TaSA-Inv* expression remained unaltered under 500 μM $LaCl_3$ or 500 μM EGTA exposure alone for 2 days but obviously decreased by about 41% and 58% for 6 days, respectively (Fig. 4C), together with insignificant alteration of *TaA/N-Inv* expression (Fig. 4D). Sucrose phosphate synthase, in conjunction with SuSy, catalyzes the production of sucrose, and SA-Inv and A/N-Inv assume the decomposition of sucrose to export carbon sources (Li et al. 2023). Sucrose synthesis and accumulation in the leaves or roots of various plants under sodium salt stress result from increased SPS and/or SuSy activities together with decreased SA-Inv activity and Inv gene expression (Yu et al. 2022; Li et al. 2023; Meng et al. 2023), and the expression of SPS and/or SuSy genes observably up-regulates in the leaves of various plants under NaCl treatment (Hu et al. 2013; Li et al. 2023). Moreover, the up-regulated expression of SuSy and SPS genes under salinity stress results in elevated sucrose level in plant roots, thus enhancing the adaptability of salt-resistant *Avena sativa* L. cultivar to salinity environment (Xu et al. 2021). The present findings confirmed that the changes of these four enzyme activities and their gene expression were responsible for restrained sucrose degradation, thus reducing energy supply and retarding seedling growth under individual NaCl, $LaCl_3$ or EGTA treatment. Different from the present observations, the notable up-regulation of SuSy gene expression under sodium salt stress is accompanied with lowered sucrose content in *Beta vulgaris* L. roots (Liu et al. 2020).

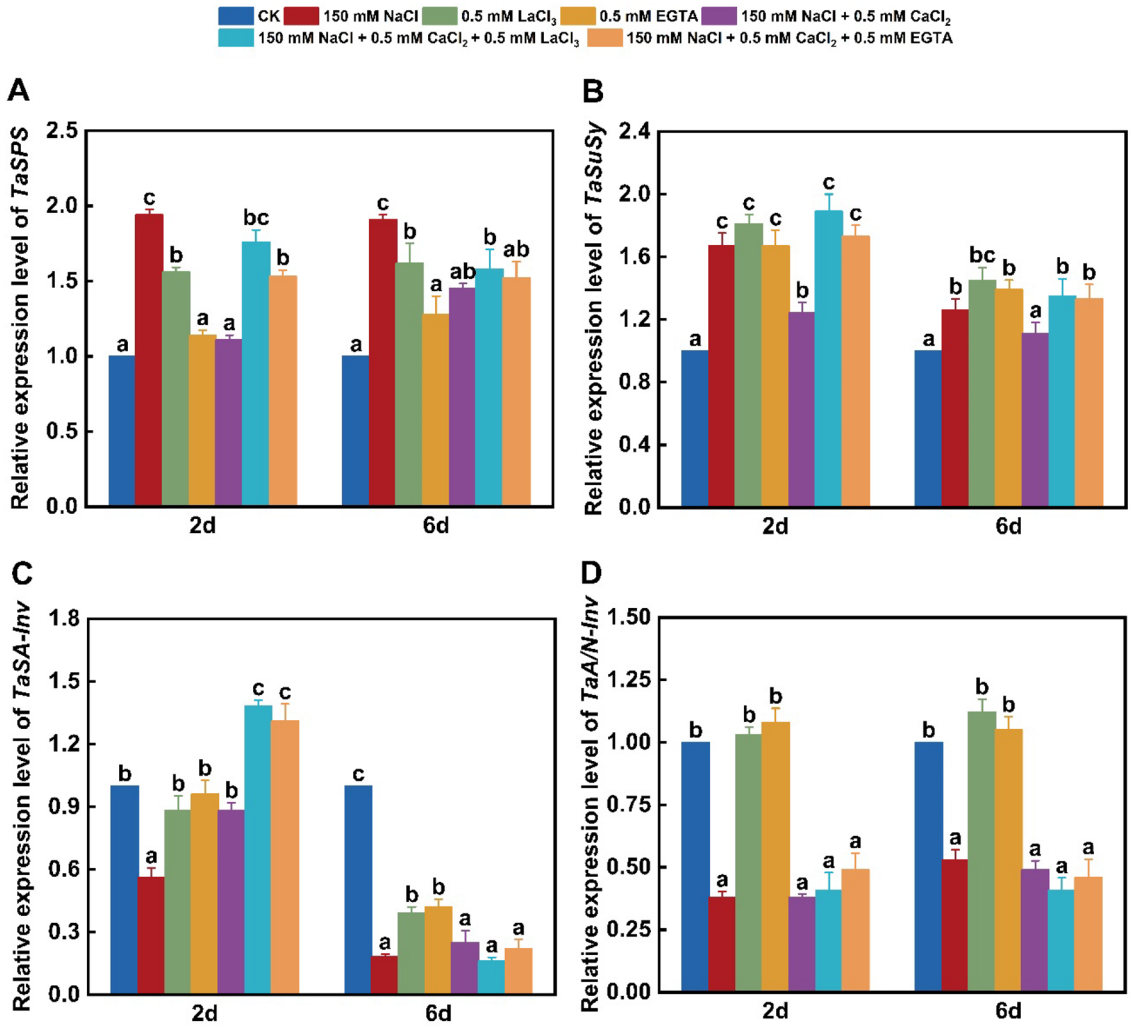

Fig. 4 Changes in gene expression related to sucrose metabolism in wheat leaves under different treatments. **A** Relative expression level of *TaSPS*; **B** relative expression level of *TaSuSy*; **C** relative expression level of *TaSA-Inv*; **D** relative expression level of *TaA/N-Inv*. Control (CK); lanthanum chloride (LaCl3); ethylene glycol tetraacetic acid (EGTA). Data are the means of three replicates (±SE). Different lowercase letters indicate significant difference between samples according to Duncan's new multiple-range test ($P < 0.05$)

The presence of 500 µM $CaCl_2$ effectively alleviated the NaCl-induced changes of SPS, SuSy, and SA-Inv activities (Fig. 3A–C). Furthermore, except for no alteration in A/N-Inv activity, adding 500 µM $LaCl_3$ or 500 µM EGTA to NaCl + $CaCl_2$-treated seedlings up-regulated SPS activity by about 20% and 84% (Fig. 3A), and SuSy activity by about 13% and 62% (Fig. 3B), along with about 13% and 10% down-regulation of SA-Inv activity (Fig. 3C), respectively, compared with 150 mM NaCl + 500 µM $CaCl_2$ treatment. Additionally, the presence of 500 µM $CaCl_2$ obviously weakened the expression of *TaSPS* by 43% and 24% and *TaSuSy* by 26% and 11% on days 2 and 6 of NaCl treatment, respectively (Fig. 4A, B). By contrast, adding 500 µM $CaCl_2$ significantly up-regulated the *TaSA-Inv* expression under sodium salt stress for 2 days but did not affect for 6 days (Fig. 4C). More importantly, adding 500 µM $LaCl_3$ or 500 µM EGTA to NaCl + $CaCl_2$-treated seedlings notably up-regulated the expression of *TaSPS* on the second day but did not alter on the sixth day (Fig. 4A), and effectively blocked the change of *TaSuSy* expression (Fig. 4B), and resulted in about 57% and 49% elevation in the relative *TaSA-Inv* expression on the second day, respectively, but unalteration on the sixth day (Fig. 4C). These changes suggested that enhanced sucrose degradation due to the up-regulation of SA-Inv activity and *TaSA-Inv* expression can supply energy for the growth of sodium salt-treated wheat seedling in the presence of $CaCl_2$. Differently, the application of exogenous calcium hydroxide and calcium nitrate upregulates SPS and SuSy activities and their gene expression but down-regulates Inv activity and its gene expression in *O. sativa* seedlings under fluorine stress (Singh et al. 2021). However, $CaCl_2$ application or combinated with $LaCl_3$ or EGTA did not alter the activity

of A/N-Inv and the expression of *TaA/N-Inv* in sodium salt-stressed seedling leaves (Figs. 3D and 4D), suggesting that the regulation of A/N-Inv activity and its gene expression in wheat leaves might be independent of Ca signaling.

Changes in CDPK and Ca^{2+}-ATPase activities and related gene expression in wheat leaves

Calcium ion (Ca^{2+}) plays pivotal roles in plant growth and responses to adverse environment. According to the above findings of this study, extracellular Ca transport and Ca signaling might be involved in the regulation of wheat seedling growth and starch and sucrose metabolism under NaCl treatment alone or combinated with $CaCl_2$. Therefore, we further analyze CDPK (a component of Ca signaling pathway) and Ca^{2+}-ATPase activities and their gene expression in wheat leaves under salinity stress alone or combinated with $CaCl_2$. Under 150 $mM{\cdot}L^{-1}$ NaCl treatment alone, CDPK activity significantly down-regulated in wheat leaves, and the activity of Ca^{2+}-ATPase also decreased to about 62% of the control (Fig. 5A, C). And also, NaCl exposure alone for 2 and 6 days obviously downregulated the expression of *TaCDPK* by about 83% and 75% (Fig. 5B) and *TaCa*$^{2+}$*-ATPase* by 77% and 78% (Fig. 5D), respectively, compared with the control. Ca^{2+}-ATPase activity is required to transfer excess Ca^{2+} out of cells or into organelles for maintaining cytoplasmic Ca^{2+} levels (Liu et al. 2014). Furthermore, salt stress-induced elevation in cytosolic Ca^{2+} is regulated by Ca^{2+}-ATPases (Sze et al. 2000), and this enzyme can be activated by binding to Ca^{2+}-CaM (Nitsche et al. 2018). Therefore, the decreased CDPK and Ca^{2+}-ATPase activities confirmed that salinity treatment blocked the Ca signal pathway and reduced cytoplasmic Ca transport in wheat leaves. Moreover, it has been indicated that the over-expression of

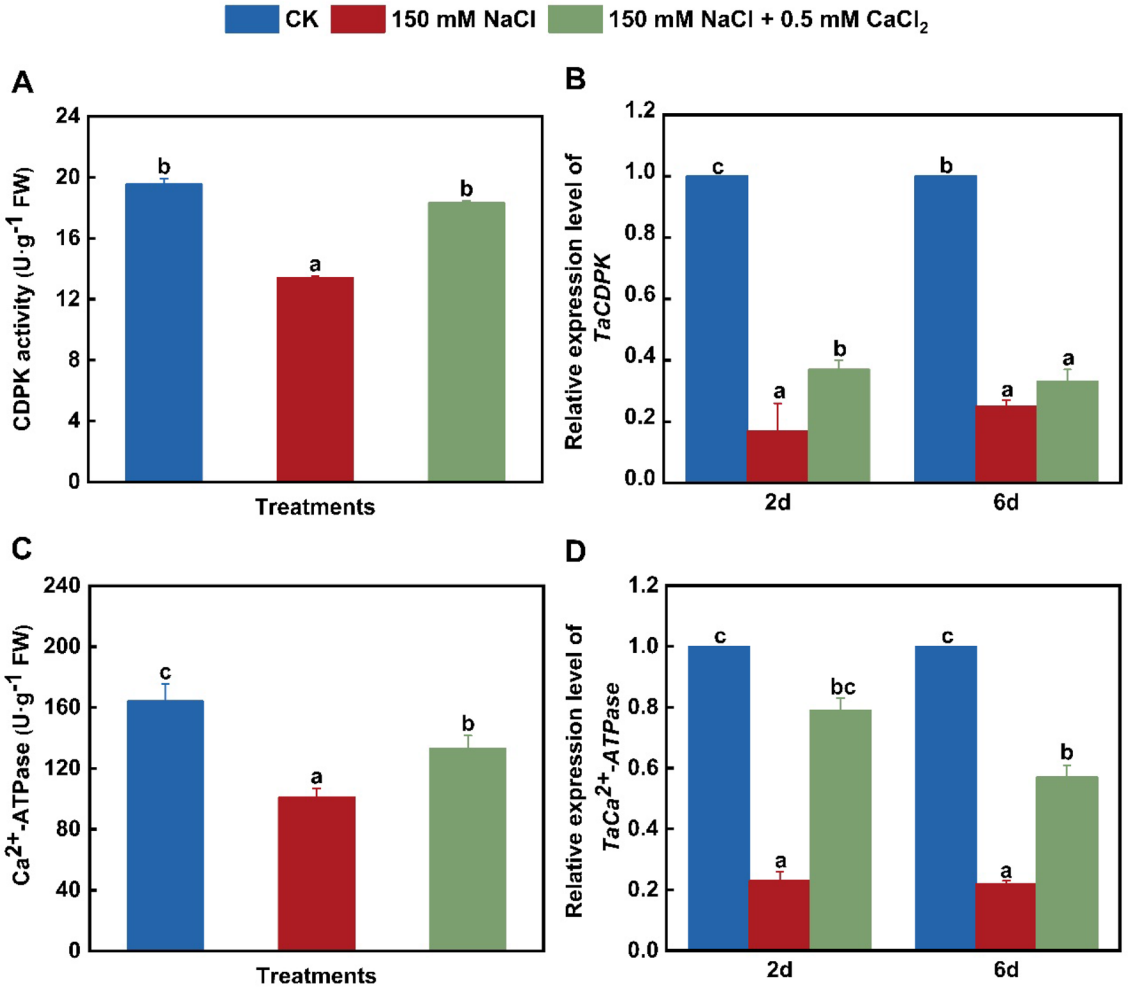

Fig. 5 Changes in CDPK and Ca^{2+}-ATPase activities and related gene expression in wheat leaves under different treatments. Control (CK). **A** Ca-dependent protein kinase (CDPK) activity; **B** relative expression level of *TaCDPK*; **C** Ca^{2+}-ATPase activity; **D** relative expression level of *TaCa*$^{2+}$*-ATPase*. Data are the means of three replicates (±SE). Different lowercase letters indicate significant difference between samples according to Duncan's new multiple-range test ($P<0.05$)

CDPK1 enhances *Arabidopsis thaliana* (L.) Heynh. tolerance to sodium salt treatment (Huang et al. 2018) and *Nicotiana tabacum* L. resistance to drought stress (Vivek et al. 2013). Therefore, the blocking of Ca signal might be the reason that salt stress inhibited the growth of wheat seedlings. However, several previous observations indicate that sodium salt stress obviously stimulates CDPK and Ca^{2+}-ATPase activity and gene expression in various plants (Wan et al. 2018; Ma et al. 2019; Zhu et al. 2021).

Exogenous Ca application up-regulates the transcription level of CDPK gene in *Cucurbita pepo* L. seedlings under nickel stress (Valivand et al. 2019) and promotes CDPK activity in *Arachis hypogaea* under sodium salt stress (Li et al. 2014). Appropriate Ca concentration also significantly enhances Ca^{2+}-ATPase gene expression in *Fagopyrum tataricum* (L.) Gaertn. seedlings under NaCl stress (Lu et al. 2021). Similar to these observations, when compared with NaCl stress alone, CDPK activity up-regulated by about 37% (Fig. 5A) and Ca^{2+}-ATPase activity notably enhanced by about 32% (Fig. 5C) under 150 $mM{\cdot}L^{-1}$ NaCl + 500 $\mu M{\cdot}L^{-1}$ $CaCl_2$ treatment. And also, adding 0.5 $mM{\cdot}L^{-1}$ $CaCl_2$ significantly promoted the expression of *TaCDPK* to 2.18 times of sodium salt treatment alone on day 2, but did not affect on day 6. Under 150 $mM{\cdot}L^{-1}$ NaCl + 0.5 $mM{\cdot}L^{-1}$ $CaCl_2$ treatment for 2 and 6 days, *TaCa*$^{2+}$*-ATPase* expression increased by about 2.43 and 1.59 folds, respectively, compared with sodium salt stress alone (Fig. 5D). These findings confirmed that the activation of intracellular Ca signal by exogenous $CaCl_2$ application was related to the up-regulation of CDPK activity and gene expression. The enhancement of Ca^{2+}-ATPase to transport Ca^{2+} could effectively blocked excess cytoplasmic Ca^{2+} accumulation in wheat leaves under sodium salt stress in the presence of $CaCl_2$. Such changes promoted wheat seedling growth. This suggestion is supported by the study of Lu et al. (2021), which demonstrated that the increased Ca^{2+}-ATPase activity medicated by exogenous Ca application is one of the reasons for the tolerant enhancement of *Solanum lycopersicum* L. seedlings to sodium salt environment (Qi et al. 2022).

Conclusion

Treatment with sodium salt, EGTA or $LaCl_3$ alone retarded wheat seedlings growth, down-regulated CDPK and Ca^{2+}-ATPase activity and their gene expression, decreased starch content but increased sucrose accumulation. Exogenous $CaCl_2$ application effectively alleviated NaCl-induced changes of these parameters in wheat leaves. Additionally, such changes of starch and sucrose metabolism were consistent with the obvious changes of related enzyme activities (Rubisco, RCA, amylase, SPS, SuSy and SA-Inv) and gene expression (*TaSPS*, *TaSuSy* and *TaSA-Inv*) in wheat leaves under different treatments. Taken together, Exogenous $CaCl_2$ application might activate the intracellular Ca messenger system and effectively triggered the synthesis of starch and the catabolism of sucrose, thereby improving wheat seedlings' tolerance to sodium salt stress.

Acknowledgements This work was financially supported by the National Natural Science Foundation of China (No. 32160749).

Author contributions YZ performed most part of the experiment and analyzed the data. DQ analyzed the data and wrote and edited. ZZ consulted and provided literature. YL and SS worked together with YZ to accomplish partial experiment. YY designed the research and edited the manuscript. In addition, YY was the corresponding author of this manuscript.

Declarations

Conflict of interest The authors declare that they have no conflict of interest.

References

Bachani J, Mahanty A, Aftab T, Kumar K (2022) Insight into calcium signalling in salt stress response. S Afr J Bot 151:1–8. https://doi.org/10.1016/j.sajb.2022.09.033

Bai QY, Yang RQ, Zhang LX, Gu ZX (2013) Salt stress induces accumulation of γ–aminobutyric acid in germinated foxtail millet (*Setaria italica* L.). Cereal Chem 90(2):145–149. https://doi.org/10.1094/CCHEM-06-12-0071-R

ElSayed AI, Mohamed AH, Rafudeen MS, Omar AA, Awad MF, Mansour E (2022) Polyamines mitigate the destructive impacts of salinity stress by enhancing photosynthetic capacity, antioxidant defense system and upregulation of Calvin cycle-related genes in rapeseed (*Brassica napus* L.). Saudi J Biol Sci 29(5):3675–3686. https://doi.org/10.1016/J.SJBS.2022.02.053

Gao JF (2006) Experimental supervision of plant physiology. Beijing, pp 100–103

Gao YL, Long RC, Kang JM, Wang Z, Zhang TJ, Sun H, Li X, Yang QC (2019) Comparative proteomic analysis reveals that antioxidant system and soluble sugar metabolism contribute to salt tolerance in alfalfa (*Medicago sativa* L.) leaves. J Proteome Res 18(1):191–203. https://doi.org/10.1021/acs.jproteome.8b00521

Hajihashemi S, Skalicky M, Brestic M, Pavla V (2020) Cross-talk between nitric oxide, hydrogen peroxide and calcium in salt-stressed *Chenopodium quinoa* Willd. at seed germination stage. Plant Physiol Biochem 154:657–664. https://doi.org/10.1016/j.plaphy.2020.07.022

Hu T, Hu LX, Zhang XZ, Zhang PP, Zhao ZJ, Fu JM (2013) Differential responses of CO_2 assimilation, carbohydrate allocation and gene expression to NaCl stress in perennial ryegrass with different salt tolerance. PLoS ONE 8(6):e66090. https://doi.org/10.1371/journal.pone.0066090

Hu W, Loka DA, Fitzsimons TR, Zhou ZG, Oosterhuis DM (2018) Potassium deficiency limits reproductive success by altering carbohydrate and protein balances in cotton (*Gossypium hirsutum* L.). Environ Exp Bot 145:87–94. https://doi.org/10.1016/j.envexpbot.2017.10.024

Huang GY, Shan CJ (2018) Lanthanum improves the antioxidant capacity in chloroplast of tomato seedlings through ascorbate-glutathione cycle under salt stress. Sci Hortic 232:264–268. https://doi.org/10.1016/j.scienta.2018.01.025

Huang K, Peng L, Liu YY, Yao RD, Liu ZB, Li XF, Yang L, Wang JM (2018) Arabidopsis calcium-dependent protein kinase *AtCPK1* plays a positive role in salt/drought-stress response. Biochem Biophys Res Commun 498(1):92–98. https://doi.org/10.1016/j.bbrc.2017.11.175

Ju FY, Pang JL, Huo YY, Zhu JJ, Yu K, Sun LY, Loka DA, Hu W, Zhou ZG, Wang SS, Chen BL, Tang QX (2021) Potassium application alleviates the negative effects of salt stress on cotton (*Gossypium hirsutum* L.) yield by improving the ionic homeostasis, photosynthetic capacity and carbohydrate metabolism of the leaf subtending the cotton boll. Field Crops Res 272:108288. https://doi.org/10.1016/J.FCR.2021.108288

Kamran M, Wang D, Xie KZ, Lu YS, Shi CH, EL Sabagh A, Gu WJ, Xu PZ (2021) Pre-sowing seed treatment with kinetin and calcium mitigates salt induced inhibition of seed germination and seedling growth of choysum (*Brassica rapa* var. *Parachinensis*). Ecotoxicol Environ Saf 227:112921. https://doi.org/10.1016/j.ecoenv.2021.112921

Ke QB, Ye J, Wang BM, Ren JH, Yin LN, Deng XP, Wang SW (2018) Melatonin mitigates salt stress in wheat seedlings by modulating polyamine metabolism. Front Plant Sci 9:914. https://doi.org/10.3389/fpls.2018.00914

Kerepesi I, Galiba G (2000) Osmotic and salt stress-induced alteration in soluble carbohydrate content in wheat seedlings. Crop Sci 40(2):482–487. https://doi.org/10.2135/cropsci2000.402482x

Kumar RR, Goswami S, Singh K, Dubey K, Singh S, Sharma R, Verma N, Kala YK, Rai GK, Grover M, Mishra DC, Singh B, Pathak H, Chinnusamy V, Rai A, Praveen S (2016) Identification of putative Rubisvo activase (*TaRca1*)-The catalytic chaperone regulating carbon assimilatory pathway in wheat (*Triticum aestivum*) under the heat stress. Front Plant Sci 7:986. https://doi.org/10.3389/fpls.2016.00986

Li XN, Jiang HD, Liu FL, Cai J, Dai TB, Cao WX, Jiang D (2013) Induction of chilling tolerance in wheat during germination by pre-soaking seed with nitric oxide and gibberellin. Plant Growth Regul 71:31–40. https://doi.org/10.1007/s10725-013-9805-8

Li Y, Fang F, Guo F, Meng JJ, Li XG, Xia GM, Wan SB (2014) Isolation and functional characterisation of CDPKs gene from *Arachis hypogaea* under salt stress. Funct Plant Biol 42(3):274–283. https://doi.org/10.1071/FP14190

Li CH, Li YH, Chu PY, Hao-hao Z, Wei ZM, Cheng Y, Liu XX, Zhao FZ, Li Y-J, Zhang ZW, Zheng Y, Mu ZS (2022a) Effects of salt stress on sucrose metabolism and growth in Chinese rose (*Rosa chinensis*). Biotechnol Biotechnol Equip 36(1):706–716. https://doi.org/10.1080/13102818.2022.2116356

Li Q, Liu R, Li ZH, Fan H, Song J (2022b) Positive effects of NaCl on the photoreaction and carbon assimilation efficiency in *Suaeda salsa*. Plant Physiol Biochem 177:32–37. https://doi.org/10.1016/J.PLAPHY.2022.02.019

Li SX, Wang Y, Gao XQ, Lan J, Fu BZ (2022c) Comparative physiological and transcriptome analysis reveal the molecular mechanism of melatonin in regulating salt tolerance in alfalfa (*Medicago sativa* L.). Front Plant Sci 13:919177. https://doi.org/10.3389/FPLS.2022.919177

Li Y, Chu Y, Yao K, Shi C, Deng X, Lin J (2023) Response of sugar metabolism in the cotyledons and roots of *Ricinus communis* subjected to salt stress. Plant Biol 25(1):62–71. https://doi.org/10.1111/plb.13475

Liu JR, Ma YN, Lv FJ, Chen J, Zhou ZG, Wang YH, Abudurezike A, Oosterhuis DM (2013) Changes of sucrose metabolism in leaf subtending to cotton boll under cool temperature due to late planting. Field Crop Res 144:200–211. https://doi.org/10.1016/j.fcr.2013.02.003

Liu W, Yuan XT, Zhang YY, Xuan YN, Yan YQ (2014) Effects of salt stress and exogenous Ca^{2+} on Na^{+} compartmentalization, ion pump activities of tonoplast and plasma membrane in *Nitraria tangutorum* Bobr. leaves. Acta Physiol Plant 36:2183–2193. https://doi.org/10.1007/s11738-014-1595-8

Liu L, Wang B, Liu D, Zou CL, Wu PR, Wang ZY, Wang YB, Li CF (2020) Transcriptomic and metabolomic analyses reveal mechanisms of adaptation to salinity in which carbon and nitrogen metabolism is altered in sugar beet roots. BMC Plant Biol 20:138. https://doi.org/10.1186/s12870-020-02349-9

Lu QH, Wang YQ, Yang HB (2021) Effect of exogenous calcium on physiological characteristics of salt tolerance in Tartary buckwheat. Biologia 76:3621–3630. https://doi.org/10.1007/s11756-021-00904-9

Ma Y, Wang P, Gu ZX, Tao Y, Shen C, Zhou YL, Han YB, Yang RQ (2019) Ca^{2+} involved in GABA signal transduction for phenolics accumulation in germinated hulless barley under NaCl stress. Food Chem X 2:100011–100023. https://doi.org/10.1016/j.fochx.2019.100023

Manishankar P, Wang NL, Köster P, Alatar AA, Kudla J (2018) Calcium signaling during salt stress and in the regulation of ion homeostasis. J Exp Bot 69(17):4215–4226. https://doi.org/10.1093/jxb/ery201

Meng FY, Feng NJ, Zheng DF, Liu ML, Zhang RJ, Huang XX, Huang AQ, Chen ZM (2023) Exogenous Hemin alleviates NaCl stress by promoting photosynthesis and carbon metabolism in rice seedlings. Sci Rep 13:3497. https://doi.org/10.1038/s41598-023-30619-7

Miceli A, Moncada A, Vetrano F (2021) Use of microbial biostimulants to increase the salinity tolerance of vegetable transplants. Agronomy 11(6):1143. https://doi.org/10.3390/agronomy11061143

Nawaz H, Manhalter S, Ali A, Ashraf MY, Lang I (2019) Ni tolerance and its distinguished amelioration by chelating agents is reflected in root radius of *B. napus* cultivars. Protoplasma 256:171–179. https://doi.org/10.1007/s00709-018-1287-0

Nitsche J, Josts I, Heidemann J, Mertens HD, Maric S, Moulin M, Haertlein M, Busch S, Forsyth VT, Svergun DI, Uetrecht C, Tidow H (2018) Structural basis for activation of plasma-membrane Ca^{2+}-ATPase by calmodulin. Commun Biol 1:206. https://doi.org/10.1038/s42003-018-0203-7

Pan JW, Li Z, Wang QG, Guan YN, Li XB, Huangfu YG, Meng FH, Li JL, Dai SJ, Liu W (2021) Phosphoproteomic profiling reveals early salt-responsive mechanisms in two foxtail millet cultivars. Front Plant Sci 12:712257. https://doi.org/10.3389/FPLS.2021.712257

Patel A, Tiwari S, Prasad SM (2023) Modulation of salt stress in paddy field cyanobacteria with exogenous application of gibberellic acid: growth behavior and antioxidative status. Physiol Mol Biol Plants 29(1):51–68. https://doi.org/10.1007/s12298-022-01266-5

Qi NN, Wang N, Hou XM, Li YH, Liao WB (2022) Involvement of calcium and calmodulin in NO-alleviated salt stress in tomato seedlings. Plants 11(19):2479. https://doi.org/10.3390/plants11192479

Qiu NW, Liu Q, Li JJ, Zhang YH, Wang FD, Gao JW (2017) Physiological and transcriptomic responses of Chinese cabbage (*Brassica rapa* L. ssp. pekinensis) to salt stress. Int J Mol Sci 18(9):1953. https://doi.org/10.3390/ijms18091953

Rekowski A, Langenkämper G, Dier M, Wimmer MA, Scherf KA, Zörb C (2021) Determination of soluble wheat protein fractions using the Bradford assay. Cereal Chem 98(5):1059–1065. https://doi.org/10.1002/cche.10447

Roy PR, Tahjib-Ul-Arif M, Polash MAS, Hossen MZ, Hossain MA (2019) Physiological mechanisms of exogenous calcium on alleviating salinity-induced stress in rice (*Oryza sativa* L.). Physiol Mol Biol Plants 25(3):611–624. https://doi.org/10.1007/s12298-019-00654-8

Seckin Dinler B, Cetinkaya H, Secgin Z (2023) The regulation of *glutathione s-transferases* by gibberellic acid application in salt treated maize leaves. Physiol Mol Biol Plants 29(1):69–85. https://doi.org/10.1007/s12298-022-01269-2

Shen JL, Wang Y, Shu S, Jahan MS, Zhong M, Wu JQ, Sun J, Guo SR (2019) Exogenous putrescine regulates leaf starch overaccumulation in cucumber under salt stress. Sci Hortic 253:99–110. https://doi.org/10.1016/j.scienta.2019.04.010

Shu HM, Zhou ZG, Xu NY, Wang YH, Zheng M (2009) Sucrose metabolism in cotton (*Gossypium hirsutum* L.) fibre under low temperature during fibre development. Eur J Agron 31(2):61–68. https://doi.org/10.1016/j.eja.2009.03.004

Singh A, Roychoudhury A, Samanta S, Banerjee A (2021) Fluoride stress-mediated regulation of tricarboxylic acid cycle and sugar metabolism in rice seedlings in absence and presence of exogenous calcium. J Plant Growth Regul 40:1579–1593. https://doi.org/10.1007/s00344-020-10202-4

Sui N, Yang Z, Liu ML, Wang BS (2015) Identification and transcriptomic profiling of genes involved in increasing sugar content during salt stress in sweet sorghum leaves. BMC Genomics 16:534. https://doi.org/10.1186/s12864-015-1760-5

Sze H, Liang F, Hwang I, Curran AC, Harper JF (2000) Diversity and regulation of plant Ca^{2+} pumps: insights from expression in yeast. Annu Rev Plant Physiol Plant Mol Biol 51:433–462. https://doi.org/10.1146/annurev.arplant.51.1.433

Valivand M, Amooaghaie R, Ahadi A (2019) Seed priming with H_2S and Ca^{2+} trigger signal memory that induces cross-adaptation against nickel stress in zucchini seedlings. Plant Physiol Biochem 143:286–298. https://doi.org/10.1016/j.plaphy.2019.09.016

Vivek PJ, Tuteja N, Soniya EV (2013) CDPK1 from ginger promotes salinity and drought stress tolerance without yield penalty by improving growth and photosynthesis in *Nicotiana tabacum*. PLoS ONE 8(10):e76392. https://doi.org/10.1371/journal.pone.0076392

Wan SQ, Wang WD, Zhou TS, Zhang YH, Chen JF, Xiao B, Yang YJ, Yu YB (2018) Transcriptomic analysis reveals the molecular mechanisms of *Camellia sinensis* in response to salt stress. Plant Growth Regul 84:481–492. https://doi.org/10.1007/s10725-017-0354-4

Wang HB, Xie F, Yao YZ, Zhao B, Xiao QQ, Pan YH, Wang HJ (2012) The effects of arsenic and induced-phytoextraction methods on photosynthesis in *Pteris* species with different arsenic-accumulating abilities. Environ Exp Bot 75:298–306. https://doi.org/10.1016/j.envexpbot.2011.08.002

Wang XC, Chang LL, Wang BC, Wang D, Li PH, Wang LM, Yi XP, Huang QX, Peng M, Guo AP (2013) Comparative proteomics of *Thellungiella halophila* leaves from plants subjected to salinity reveals the importance of chloroplastic starch and soluble sugars in halophyte salt tolerance. Mol Cell Proteom 12(8):2174–2195. https://doi.org/10.1074/mcp.M112.022475

Wei MY, Liu JY, Li H, Hu WJ, Shen ZJ, Qiao F, Zhu CQ, Chen J, Liu X, Zheng HL (2021) Proteomic analysis reveals the protective role of exogenous hydrogen sulfide against salt stress in rice seedlings. Nitric Oxide 111–112:14–30. https://doi.org/10.1016/J.NIOX.2021.04.002

Winter H, Huber SC (2000) Regulation of sucrose metabolism in higher plants: localization and regulation of activity of key enzymes. Crit Rev Plant Sci 19(1):31–67. https://doi.org/10.1080/07352680091139178

Xia XJ, Huang LF, Zhou YH, Mao WH, Shi K, Wu JX, Asami T, Chen ZX, Yu JQ (2009) Brassinosteroids promote photosynthesis and growth by enhancing activation of Rubisco and expression of photosynthetic genes in *Cucumis sativus*. Planta 230:1185–1196. https://doi.org/10.1007/s00425-009-1016-1

Xing YF, Chen XF, Zhang M, Bang Li, Cui T, Liu C, Liu CJ, Chen BR, Zhou YF (2023) $CaCl_2$ priming promotes sorghum seed germination under salt stress by activating sugar metabolism. Plant Growth Regul 101:385–397. https://doi.org/10.1007/s10725-023-01025-w

Xu ZS, Chen XJ, Lu XP, Zhao BP, Yang YM, Liu JH (2021) Integrative analysis of transcriptome and metabolome reveal mechanism of tolerance to salt stress in oat (*Avena sativa* L.). Plant Physiol Biochem 160:315–328. https://doi.org/10.1016/J.PLAPHY.2021.01.027

Yan FY, Zhang JY, Li WW, Ding YF, Zhong QY, Xu X, Wei HM, Li GH (2021) Exogenous melatonin alleviates salt stress by improving leaf photosynthesis in rice seedlings. Plant Physiol Biochem 163:367–375. https://doi.org/10.1016/J.PLAPHY.2021.03.058

Yang YL, Wei XL, Shi RY, Fan Q, An LZ (2010) Salinity-induced physiological modification in the callus from halophyte *Nitraria tangutorum* Bobr. J Plant Growth Regul 29:465–476. https://doi.org/10.1007/s00344-010-9158-8

Yang Y, Xie JM, Li J, Zhang J, Zhang XD, Yao YD, Wang C, Niu TH, Bakpa EP (2022) Trehalose alleviates salt tolerance by improving photosynthetic performance and maintaining mineral ion homeostasis in tomato plants. Front Plant Sci 13:974507. https://doi.org/10.3389/FPLS.2022.974507

Yu QL, Sun WJ, Han YY, Hao JH, Qin XX, Liu CJ, Fan SX (2022) Exogenous spermidine improves the sucrose metabolism of lettuce to resist high-temperature stress. Plant Growth Regul 96:497–509. https://doi.org/10.1007/S10725-022-00800-5

Zhang LN, Xie JQ, Wang LT, Si LB, Zheng S, Yang YL, Yang H, Tian SG (2020) Wheat *TabZIP8*, *9*, *13* participate in ABA biosynthesis in NaCl-stressed roots regulated by *TaCDPK9-1*. Plant Physiol Biochem 151:650–658. https://doi.org/10.1016/j.plaphy.2020.03.039

Zhang Y, Li GY, Si LB, Liu N, Gao TP, Yang YL (2021) Effects of tea polyphenols on the activities of antioxidant enzymes and the expression of related gene in the leaves of wheat seedlings under salt stress. Environ Sci Pollut Res 28:65447–65461. https://doi.org/10.1007/S11356-021-15492-Z

Zhang XH, Ma C, Zhang L, Su M, Wang J, Zheng S, Zhang TG (2022) GR24-mediated enhancement of salt tolerance and roles of H_2O_2 and Ca^{2+} in regulating this enhancement in cucumber. J Plant Physiol 270:153640. https://doi.org/10.1016/j.jplph.2022.153640

Zhang XY, He PY, Guo RY, Huang KF, Huang XY (2023) Effects of salt stress on root morphology, carbon and nitrogen metabolism, and yield of Tartary buckwheat. Sci Rep 13:12483. https://doi.org/10.1038/s41598-023-39634-0

Zhu YX, Guo J, Feng R, Jia JH, Han WH, Gong HJ (2016) The regulatory role of silicon on carbohydrate metabolism in *Cucumis sativus* L. under salt stress. Plant Soil 406:231–249. https://doi.org/10.1007/s11104-016-2877-2

Zhu HY, He MW, Jahan MS, Wu JQ, Gu QS, Shu S, Sun J, Guo SR (2021) CsCDPK6, a CsSAMS1-interacting protein, affects polyamine/ethylene biosynthesis in cucumber and enhances salt tolerance by overexpression in tobacco. Int J Mol Sci 22(20):11133. https://doi.org/10.3390/ijms222011133